Developmental Cognitive Neuroscience 58 (2022) 101171

Contents lists available at ScienceDirect

Developmental Cognitive Neuroscience

journal homepage: www.elsevier.com/locate/dcn

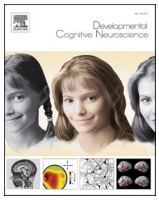

Longitudinal developmental trajectories of inhibition and white-matter maturation of the fronto-basal-ganglia circuits

Mervyn Singh [a,b,*], Patrick Skippen [c], Jason He [d], Phoebe Thomson [e,f], Ian Fuelscher [a,b], Karen Caeyenberghs [a,b], Vicki Anderson [e,f,g], Jan M. Nicholson [h], Christian Hyde [a,b], Timothy J. Silk [a,b,e]

[a] Cognitive Neuroscience Unit, School of Psychology, Deakin University, Geelong, Victoria, Australia
[b] Centre for Social and Early Emotional Development, Deakin University, Geelong, Victoria, Australia
[c] Neuroscience Research Australia, Randwick, NSW 2031, Australia
[d] Department of Forensic and Neurodevelopmental Sciences, Sackler Institute for Translational Neurodevelopment, Institute of Psychiatry, Psychology, and Neuroscience, King's College London, London, UK
[e] Developmental Imaging, Murdoch Children's Research Institute, Melbourne, Victoria, Australia
[f] Department of Paediatrics, University of Melbourne, Melbourne, Victoria, Australia
[g] The Royal Children's Hospital, Melbourne, Australia
[h] Judith Lumley Centre, La Trobe University, Melbourne, Australia

ARTICLE INFO

Keywords:
Fixel-based analysis
Diffusion MRI
Childhood Development
Response inhibition
Stop-signal task
Longitudinal analyses

ABSTRACT

Response inhibition refers to the cancelling of planned (or restraining of ongoing) actions and is required in much of our everyday life. Response inhibition appears to improve dramatically in early development and plateau in adolescence. The fronto-basal-ganglia network has long been shown to predict individual differences in the ability to enact response inhibition. In the current study, we examined whether developmental trajectories of fiber-specific white matter properties of the fronto-basal-ganglia network was predictive of parallel developmental trajectories of response inhibition. 138 children aged 9–14 completed the stop-signal task (SST). A subsample of 73 children underwent high-angular resolution diffusion MRI data for up to three time points. Performance on the SST was assessed using a parametric race modelling approach. White matter organization of the fronto-basal-ganglia circuit was estimated using fixel-based analysis. Contrary to predictions, we did not find any significant associations between maturational trajectories of fronto-basal-ganglia white matter and developmental improvements in SST performance. Findings suggest that the development of white matter organization of the fronto-basal-ganglia and development of stopping performance follow distinct maturational trajectories.

1. Introduction

The cancelling of planned or ongoing actions, known as response inhibition, has long been recognized as critical for efficient behavioral regulation in an ever-changing world (Bari and Robbins, 2013; Lipszyc and Schachar, 2010). Difficulties with response inhibition are often also observed in individuals with developmental disorders such as attention-deficit hyperactivity disorder (ADHD; Anzman-Frasca et al., 2015; Schachar et al., 2007). Despite this, the behavioral and neural mechanisms underlying the development of response inhibition during childhood and adolescence remain unclear.

In experimental settings, response inhibition is commonly assessed using the Stop-signal Task (SST), a paradigm in which participants make speeded responses to a series of forced-choice discrimination trials (go trials) whilst inhibiting their prepotent responses on a subset of trials (stop trials) when prompted by a stop-signal (Matzke et al., 2018; Verbruggen and Logan, 2008). The prominent horse-race model (Logan and Cowan, 1984; Verbruggen and Logan, 2009) conceptualizes SST performance as a race between two processes: (1) a go process that is triggered by the onset of a go stimulus, and (2) a stop process triggered by the stop-signal. Inhibitory control during stop trials is ultimately determined as the outcome of this race. If the stop process is adequately

* Correspondence to: Cognitive Neuroscience Unit, School of Psychology, Deakin University, 221 Burwood Highway, Burwood, VIC 3125, Australia.
E-mail address: mervyn.singh@deakin.edu.au (M. Singh).

https://doi.org/10.1016/j.dcn.2022.101171
Received 30 May 2022; Received in revised form 6 October 2022; Accepted 29 October 2022
Available online 31 October 2022

engaged at the onset of the stop-signal, it has enough time to 'overtake' the go process, resulting in successful inhibition of the prepotent response (Logan and Cowan, 1984). The horse-race model thus operationalizes response inhibition as a stop-signal reaction time (SSRT), reflecting the otherwise unobservable latency of the stop process (Matzke et al., 2018). SSRTs are traditionally indexed as single measures (i.e., mean), with lower values indicative of better response inhibition efficiency (Verbruggen and Logan, 2008).

Response inhibition has been demonstrated to undergo continuous improvement throughout early childhood and adolescence (Bedard et al., 2002; Curley et al., 2018; Dupuis et al., 2019; Madsen, 2010; Madsen et al., 2020; Williams et al., 1999). Prior developmental work in healthy children has shown rapid decreases in SSRT during early childhood, reaching a peak in adolescence before plateauing (Curley et al., 2018; Madsen et al., 2020). However, the use of single estimates of inhibitory ability (i.e., mean SSRT) has been criticized as being limited at capturing interindividual differences in performance variability (Matzke et al., 2013; Verbruggen et al., 2013). Recent neurophysiological models of response inhibition posit that successful stopping is concomitant on a range of peripheral cognitive mechanisms, such as stimulus detection and attentional monitoring (Diesburg and Wessel, 2021; Jana et al., 2020; Skippen, 2019). Performance differences in SSRTs may reflect a general variability in the recruitment of these other broader cognitive processes, rather than inhibition more specifically. The predominant use of SSRTs, especially in the developmental literature, may conceal these crucial features of the data, resulting in inaccurate interpretations about the nature of inhibitory improvements in childhood.

A large body of neuroimaging work has linked response inhibition in the SST to white matter properties of the fronto-basal-ganglia circuit, a triad of tracts connecting the inferior frontal gyrus (IFG), presupplementary motor area (preSMA) and the subthalamic nucleus (STN) (Aron et al., 2016, 2007; Hannah and Aron, 2021). Indeed, studies employing Diffusion Tensor Imaging (DTI), a popular method of quantifying the direction of water diffusion across white matter axons (O'Donnell and Westin, 2011), have demonstrated significant associations between reduced SSRT in children and greater white matter coherence (indexed as increased fractional anisotropy; FA and lower mean diffusivity; MD) within the fronto-basal-ganglia circuit (Madsen, 2010). Nevertheless, much of the above work has been conducted in cross-sectional samples and hence are unable to fully characterize the direction of the relationship between brain structure and behavioral function. To our knowledge, only one study has looked at the developmental course of white matter underlying fronto-basal-ganglia circuitry, and its relation to the maturation of response inhibition. Madsen and colleagues (2020) observed that faster SSRTs in childhood (7–19 years, $N = 88$) were contingent on the degree of change in fractional anisotropy (FA) within the right preSMA. More specifically, children with lower-than-average FA in the right preSMA at baseline exhibited a developmental lag in inhibitory performance at earlier ages compared to those with higher-than-average FA. However, this study, and the majority of the cross-sectional work, has used DTI-based measures which are non-specific to the biophysical properties underlying white matter (Farquharson et al., 2013; Jeurissen et al., 2013). Thus, the nature of the relationship between developmental changes in the fronto-basal-ganglia circuit and response inhibition remains unclear.

The advent of higher-order diffusion models allow greater biological specificity to which white matter microstructure can be quantified, especially in the presence of crossing fibres (Dell'Acqua and Tournier, 2019; Tournier et al., 2007). To address the pitfalls of the prevailing DTI method, our team recently leveraged Fixel-based analysis (FBA) (Dhollander et al., 2021; Raffelt et al., 2017), a higher-order analytical framework, to re-examine the relationship between fronto-basal-ganglia microstructure and response inhibition in children aged 9–11 (Singh et al., 2021). FBA encodes white matter properties at the fixel level, allowing for specific fibre properties within voxels to be quantified with greater biological specificity compared to DTI (Dhollander et al., 2021). Metrics that can be derived from FBA include: (i) fibre density (FD), a microstructural measure of local axonal density, and (ii) fibre cross-section (FC), a morphological estimate of fibre bundle size (Raffelt et al., 2012, 2017). Using FBA, we revealed that better inhibitory control (lower SSRT) was largely facilitated by greater FD in the subcortical projections of the right and left IFG-STN and preSMA-STN pathways, suggesting that microstructural alterations in these tracts may be a crucial factor in distinguishing individual differences in stopping performance in children (Singh et al., 2021). Nevertheless, as this study was also conducted using a cross-sectional approach, interpretations of how these patterns may be reflected across development remain unknown. Independent of inhibition, longitudinal FBA studies have shown widespread increases in both FD and FC across several white matter tracts related to executive and sensorimotor functioning such as the superior longitudinal fasciculus and corpus callosum (Dimond et al., 2020; Genc et al., 2020, 2018). The methodological advantages of the FBA framework therefore is an ideal candidate with which to probe the developmental trajectories of fronto-basal-ganglia white matter and response inhibition.

In the present study, we aimed to determine: (1) the development of response inhibition over ages 9–14; (2) white matter maturation of within the fronto-basal-ganglia circuit, and (3) whether developmental changes in the white matter properties of the fronto-basal-ganglia circuit predicted changes in response inhibition. In line with previous response inhibition work (Curley et al., 2018; Dupuis et al., 2019; Madsen et al., 2020; Williams et al., 1999), we hypothesized that response inhibition (as indexed by SSRT) would be significantly associated with age. However, given the limitations of traditional SSRT, our next aim was to disentangle the features of the SSRT distribution that contribute to performance variability. Here we employed the parametric race-model, a bespoke approach which estimates the entire distribution of SSRTs, rather than just the mean found in traditional non-parametric models (Matzke et al., 2013). The parametric-race model assumes parameters (e.g., SSRT) follow the shape of an ex-Gaussian distribution and are characterized by the mean (mu), standard deviation (sigma), and the exponential 'tail' (tau) of the distribution (Dawson, 1988; Matzke et al., 2013). Thus, the parametric race model affords a more fine-grained assessment of the specific components underlying the SSRT distribution. Here, we hypothesized that age-related improvements in SSRT would be paralleled by reductions in the overall mean of the response times (mu), response variability (sigma) and the propensity to engage in late responses across stop-trials (tau). These effects were expected given previous developmental evidence showing that as children age, their consistency and ability to inhibit prepotent motor responses more quickly, improves (Williams et al., 2005, 1999).

Second, reflecting evidence of brain white matter maturation in childhood (Lebel et al., 2019), we applied FBA to explore the developmental progression of fiber specific properties within the fronto-basal-ganglia circuit. FBA was chosen as it provides biologically specific metrics that account for the presence of complex fiber orientations in white matter (Dhollander et al., 2021). Here, we hypothesized that fronto-basal-ganglia white matter microstructure (fiber density; FD), and morphology (fiber cross-section; FC) would increase with age. Lastly, considering DTI-based evidence linking improvements in inhibitory control to alterations in fronto-basal-ganglia white matter (Madsen et al., 2020), we hypothesized that greater FD and FC will be associated with developmental improvements on SST task performance.

2. Methods

2.1. Participants

This study reports on a cohort of children aged 9–14 from the Neuroimaging of the Children's Attention Project (NICAP) (Silk et al., 2016). NICAP is a community-based cohort of children with and without

ADHD. Given that the aim of the present work was to examine the development of response inhibition and fronto-basal-ganglia white matter in a non-clinical population, we therefore excluded participants at each of the three timepoints with a confirmed diagnosis of ADHD. Informed consent was obtained from parents and/or guardians prior to children participating in the study. For the present work, we identified participants who had completed the SST for at least one, and up to three time points. Participants underwent up to 3 repeated assessments (time points 1–3) between the ages of 9–14 years. For our neuroimaging subsample, we further identified participants from the total behavioral sample who had diffusion MRI data for up to three time points. Socio-economic status (SES) was assessed at all three timepoints using the Index of Relative Socio-economic Advantage and Disadvantage (IRSAD) (Australian Bureau of Statistics, 2013). Briefly, the IRSAD is a measure of relative socio-economic disadvantage in Australia. The IRSAD has a mean of 1000 and a standard deviation of 100, and areas are on a continuum from most disadvantaged to most advantaged relative to the mean. Lower IRSAD SES scores indicate areas with greater incidence of disadvantage, whilst the opposite is true for higher IRSAD scores. To ensure that the community sample was reflective of the general population, participants were sourced from 43 schools spanning multiple socioeconomic strata across Eastern and Western Melbourne. Intelligence Quotients (IQ) were also obtained at baseline using the Wechsler Abbreviated Scale of Intelligence (Wechsler, 1999).

Following data cleaning and quality-control assessment of the behavioral (Appendix A, Supplementary Section S.2) and neuroimaging data (Appendix A, Supplementary Section S.4), the final behavioral sample comprised of 138 participants aged 9–14 years (83 completed one time point, 39 completed two time points, and 16 completed all three time points). The final neuroimaging sample comprised of 116 scans from 73 participants. (38 were only scanned once, 27 were scanned twice, and 8 were scanned thrice. A visual representation of the distribution of participants at each assessment point for the behavioral and neuroimaging samples is presented in Fig. 1, panels A and B respectively. A flow chart of the data analysis pipeline is illustrated in Fig. 2. Detailed information on all methodological steps can be found in the Supplementary Materials (Appendix A).

Attrition analyses were conducted in both behavioral and neuroimaging cohorts to examine potential biases in key demographic (IQ; SES) and SST measures (SSRT; mu, sigma, and tau of the stop-trial distribution) across participants who completed either one, two or three timepoints. Results revealed no significant differences between individuals attending one, two or three timepoints in any of the demographic or SST measures of interest (behavioral sample p range = 0.521–0.932; neuroimaging sample p range = 0.318–0.849), suggesting that no biases due to attrition exist in the data. For further details on the attrition analyses, please consult Section S.5 of Appendix A.

2.2. *Cognitive Assessment: Stop-signal Task*

Participants completed a 3.5-hour behavioral assessment at the Murdoch's Children Research Institute in Melbourne, Australia for each of the three time points. Assessment measures comprised of a cognitive battery (which included the SST), a self-report survey, and a parent questionnaire. Response inhibition was assessed using the STOP-IT version of the SST which is freely available for download for Windows (Verbruggen et al., 2008). Further details on task design and characteristics can be found in Section 1 of the Supplementary Materials (Appendix A).

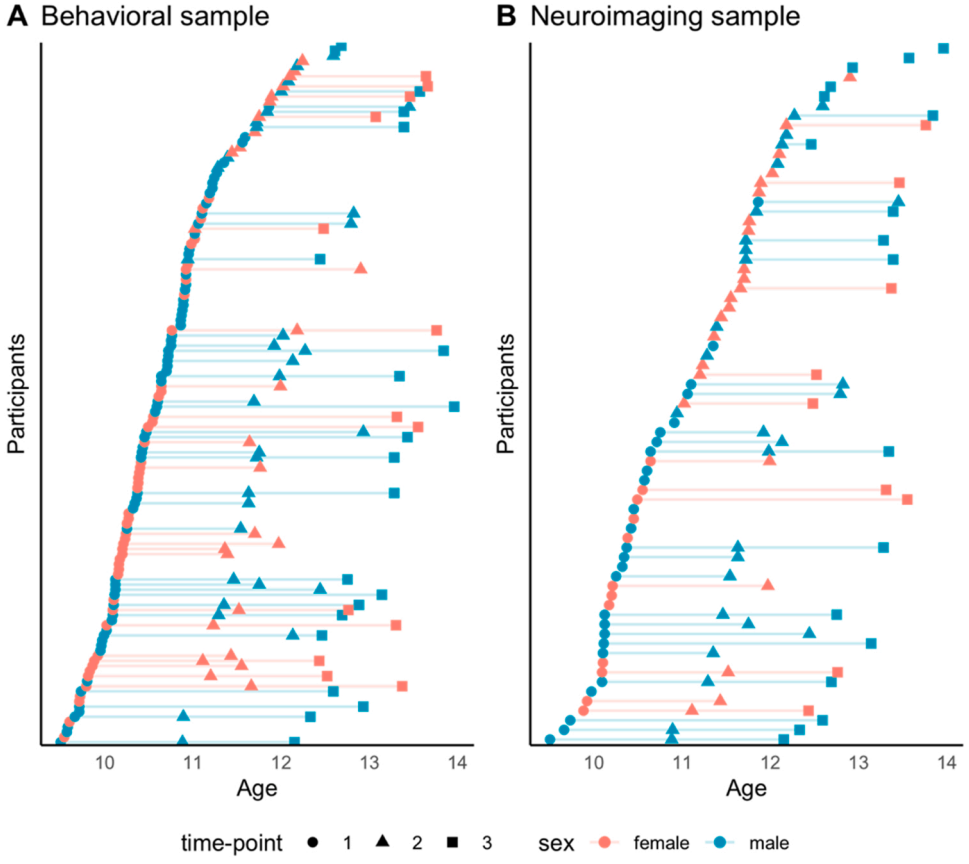

Fig. 1. (A) Distribution of scores for each subject in the behavioral sample (N = 138); (B) Distribution of scores for each subject in the neuroimaging sample (N = 73). Subjects are ordered by age (years).

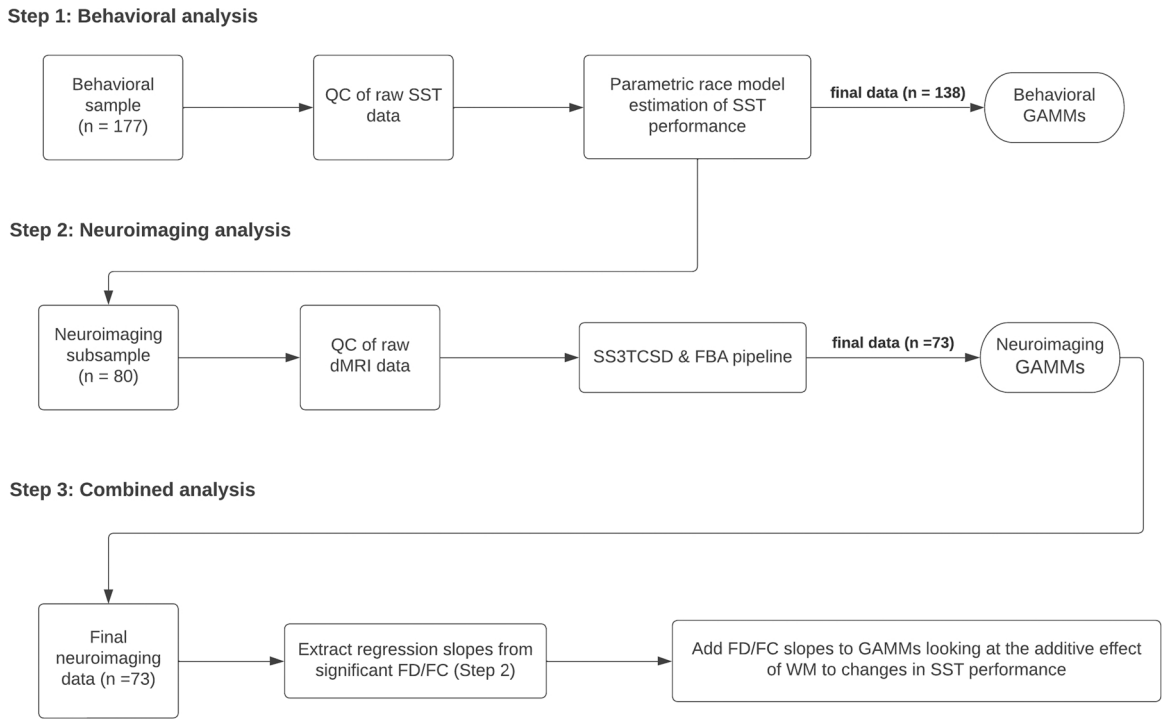

Fig. 2. Basic flow diagram of the analysis procedures undertaken in the present study. Detailed information on each step of the process is presented in the Methods and the Supplementary Materials (Appendix A). Note: SST: Stop-signal Task; QC: Quality Control; GAMMs: Generalized additive mixed-models; dMRI: Diffusion MRI; SS3TCSD: Single-shelled three-tissue constrained spherical deconvolution; FBA: Fixel-based Analysis; FD: Fiber density; FC: Fiber cross-section.

2.3. Parametric estimation of response inhibition

Quantitative measures of response inhibition were derived by fitting raw subject-level data to the parametric race-model, resulting in separate parameters that quantify the mean (muS), variability (sigmaS), and exponential tail (tauS) of the stopping distribution (Matzke et al., 2019). Prior to parametric estimation, raw SST data were appraised so that only participants who adequately completed the task entered the final analyses. Details of the quality control procedure can be found in Section S.2 of Appendix A and Table S1 of Appendix B. Briefly, participants were excluded if they did not (i) complete the task; (ii) slowed their go RT by more than 300 ms over the course of the task; (iii) reported a stop response rate of $>$ 75 %, and (iv) reported no errors on go-trials (100 % accuracy). Further, we visually inspected each participant's probability of responding to a stop-signal to assess if they retained a 50 % success rate. Summary estimates (means) were computed for all individual-subject level parameters for use in subsequent analyses. Lastly, to facilitate comparability of our work with those of previous studies (Curley et al., 2018; Madsen et al., 2020), traditional SSRT estimates were computed for each subject by adding mu and tau parameters of the stopping distribution. All steps of the parametric race-model were conducted in R (v.4.0.3) using the Dynamic models of Choice package (https://osf.io/pbwx8/). Detailed information can be found in Section 3 of the Supplementary Materials (Appendix A).

2.4. Neuroimaging: Diffusion & T1-weighted MRI

Diffusion-weighted and T1-weighted MRI images were acquired on a 3 T Siemens MRI scanning system at a single site across three time points (see Section S.4.1 of Appendix A for acquisition parameters). Data for time points 1 and 2 were acquired on a TIM Trio scanner whilst data for time point 3 were acquired following an upgrade to the MAGNETOM Prisma scanner. The effect of scanner type is accounted for in subsequent statistical analysis. Following the recommended pre-processing pipeline for single-shelled diffusion data (Tournier et al., 2019), diffusion images were quality checked and were removed if the pre-processing step failed, or if data quality was insufficient for further analysis (i.e., masking issues or hyperintense regions). Further details of the quality control procedure can be found in Section S.4.2 of Appendix A and Table S2 of Appendix B.

Fixel-based Analysis (FBA) was conducted following the approach recommended for single-shelled 3-tissue Constrained spherical deconvolution (SS3T-CSD) (Dhollander and Connelly, 2016). Regions-of-interest (ROIs) implicated in the fronto-basal-ganglia circuit (inferior frontal gyrus [IFG], presupplementary motor area [preSMA] and subthalamic nucleus [STN]) were parcellated from each subject's T1-weighted image following the approach in our baseline cross-sectional study (Singh et al., 2021). Full details of our parcellation scheme and ROI placement can be accessed in the relevant manuscript and in Section S.4.4 of Appendix A. Probabilistic tractography was then applied bilaterally to obtain white matter tracts of the fronto-basal-ganglia circuit in a pairwise fashion (See Fig. 3). Tracts in each hemisphere were segmented into fixel masks and mean fiber density (FD) and fiber cross-section (FC) were computed across all fixels to quantify micro- and macrostructural properties respectively. Given that FC values are often typically skewed, FC was further log-transformed (logFC) to ensure normal distribution of the data in the analysis as per the recommended FBA pipeline (Dhollander et al., 2021). Lastly, head motion and total brain volume were calculated as mean framewise displacement (FWD) and mean estimated total intracranial volume (eTIV) respectively (Table 3) (Power et al., 2012; Smith et al., 2019).

All steps of the FBA pipeline were performed in Mrtrix3Tissue (v5.2.8; https://3tissue.github.io/), a fork of the Mrtrix3 software package (Tournier et al., 2019). Computational resources were provided by the MASSIVE high-performance computing cluster (Goscinski et al., 2014). For further details on all steps in the FBA pipeline, see Supplemental Section 4 (Appendix A).

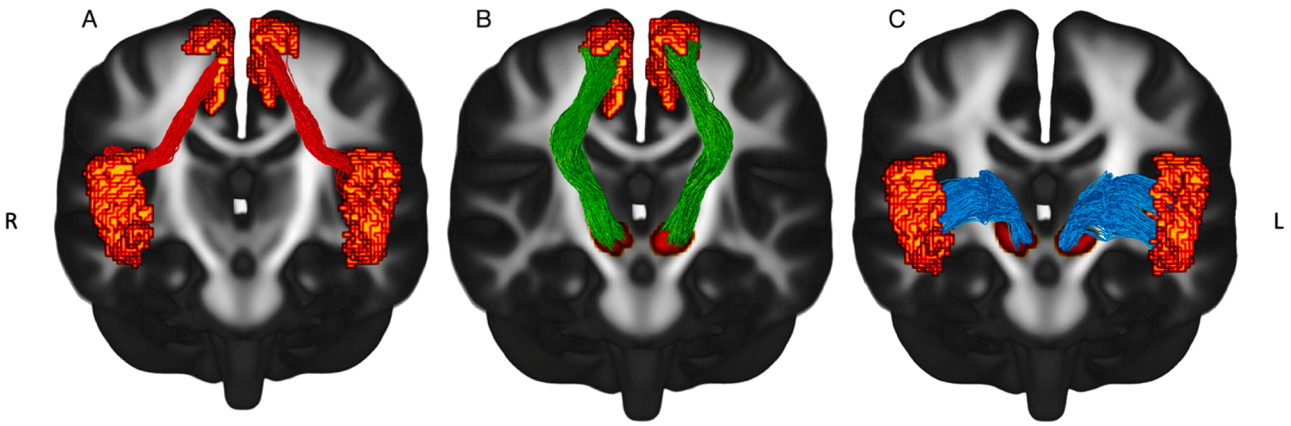

Fig. 3. Tracts of the fronto-basal-ganglia circuit. (A) Bilateral IFG-preSMA pathway; (B) bilateral preSMA-STN pathway; (C) bilateral IFG-STN pathway. Voxel position of each coronal slice in millimetres: x = 0, y = −8.5, z = 18.

2.5. Primary analysis

Longitudinal analyses were conducted using generalized additive mixed models (GAMMs) in the 'mgcv' package in R (v1.8.34) (Wood, 2011). GAMMs were chosen as the preferred method of assessing developmental trajectories due to their flexibility in accounting for nonlinear relationships between variables (Hastie and Tibshirani, 1990; Wood, 2017). Starting from a baseline null model, models of increasing complexity were iteratively added in a stepwise fashion. Based on prior recommendations (Wood, 2017), all models were fitted using the maximum likelihood (ML) estimation method (Wood, 2011), with a penalized cubic regression spline and basis dimension of 4. Lastly, all continuous predictors were mean centered to improve interpretability of the intercepts. Model comparisons were conducted between the current and next model in the iteration using a combination of fit statistics. First, we considered the difference in the Akaike Information criterion (AIC) values between models. Recent studies suggest that the AIC is the most appropriate fit statistic for identifying the model closest to the true model, with lower AIC values indicating better fit between the observed and true model (Lewis et al., 2011; Portet, 2020). In addition, the significance of the best-fitting model was assessed by performing a chi-square test on two times the difference in minimized smoothing parameter selection scores, and the difference in degrees of freedom between two models (Van Rij et al., 2015). A p-value of < 0.05 indicates the more complex model provided better fit to the data than the less complex model. Based on these criteria, more complex models in the iteration were chosen if the following were met: (1) chi-square test was significant ($p < .05$); (2) the AIC difference between the current and next model is ≥ 2, with the AIC of the complex model being smaller than the previous model.

2.5.1. Developmental trajectories of SST performance

Developmental trajectories of response inhibition were assessed by conducting a series of GAMMs (Appendix A, Section 5, Table S2) examining whether age-at-assessment, sex, and the interaction between age and sex significantly predicted individual changes in mu, sigma, and tau of the SSRT distribution. Further, to facilitate comparability of our work with those of previous studies (Madsen et al., 2020), we also modelled the longitudinal trajectories of response inhibition using traditional SSRT. Sex effects were explored given recent evidence suggesting that sex differences may underlie performance variability in response inhibition (Ribeiro et al., 2021; Rubia et al., 2013). Participant ID was entered into all models as a random effect to account for individual differences in subject-level intercepts (Gibbons et al., 2010). We also adjusted for SES as there is evidence suggesting that it can impact executive functioning development (Last et al., 2018; Lawson et al., 2018). Best-fitting models (identified using the approach detailed in Section 2.5) were then used as the initial 'null' model in our analysis examining the association between response inhibition and fronto-basal-ganglia white matter (Section 2.5.3).

2.5.2. Developmental trajectories of fronto-basal-ganglia white matter organization

Maturational changes in fronto-basal-ganglia white matter were assessed by computing GAMMs for each FBA metric in our neuroimaging subsample (Appendix A, Section 5, Table S3). Like our behavioral analysis, a series of models were tested to examine whether age-at-assessment, sex, and the interaction between age and sex significantly predicted developmental trajectories in FD or logFC in the IFG-preSMA, IFG-STN and preSMA-STN pathways. All models were conducted using the same parameters as those described for the behavioral analyses (see Section 2.5). In addition to controlling for SES and subject-level intercepts, we also adjusted for the following: (1) head size (eTIV), (2) head motion (FWD), and (3) scanner type, across all models. Mean eTIV was adjusted since changes in white-matter organization are often sensitized to gross variations in brain size (Smith et al., 2019). If unaccounted for, it is difficult to ascertain if developmental trajectories in FC are indicative of a true effect or driven by general volumetric differences. Since our sample consists of children aged 9–14, this is especially pertinent since the transition to adolescence is marked by large-scale changes in brain structure (Lebel et al., 2019). Considering previous evidence that the fronto-basal-basal-ganglia circuit may be right lateralized during inhibitory control (Aron et al., 2016; Madsen, 2010), models were run separately for the left and right hemisphere. Due to the large number of comparisons performed during statistical modelling, p-values were adjusted for Type 1 error by using the false discovery rate method (p_{FDR}) (Benjamini and Hochberg, 1995) at 0.05. All corrections for multiple comparisons were conducted using the 'p. adjust' function in R. Tracts that show a significant age-related change in FD/FC were included as predictors in the third analysis (Section 2.5.3).

2.5.3. Associations between fronto-basal-ganglia white matter and SST performance

This analysis extends models from section 2.5.1 to determine whether developmental patterns of SST performance (as observed in our behavioral-only GAMMs) are predicted by fronto-basal-ganglia white matter maturational changes (Appendix A, Section 5, Table S4). To obtain our measures of change in FD/FC, random age slopes from linear mixed effects models were extracted based on a model predicting fronto-basal-ganglia white matter from age (adjusting for FWD and eTIV). Steeper slopes indicate a greater increase in FD or FC with age. These slopes were added as predictors in a sequence of GAMMs predicting developmental trajectories in response inhibition. Specifically, we ran a (1) baseline 'null' model which is the initial best-fitting model for the

Table 1
Summary characteristics for all variables in the behavioral sample (N = 138).

	T1 (n = 115)	T2 (n = 60)	T3 (n = 34)
Demographics			
Sex, % female	42	45	38
Hand, % right	88	88	85
Age, mean (SD)	10.5 (0.5)	11.8 (0.5)	13.1 (0.5)
IQ, mean (SD)	102.2 (14.1)	101.1 (12.8)	100.6 (11.7)
SES, mean (SD)	1021 (43)	1025 (46)	1016 (40)
SST performance (ms)			
muS, mean (SD)	151.91 (62.90)	139.05 (38.88)	151.55 (44.23)
sigmaS, mean, (SD)	190.58 (93.97)	141.96 (87.55)	139.74 (94.73)
tauS, mean (SD)	148.66 (63.42)	110.06 (54.72)	102.37 (57.09)
SSRT, mean (SD)	317.81 (102.30)	262.59 (71.22)	266.24 (70.13)

Note: SD: Standard deviation; IQ: Intelligence Quotient; SES: Socioeconomic status; SSRT: Stop-signal reaction time; MuS: Mu of the stop-signal reaction time distribution; SigmaS: Sigma of the stop-signal reaction time distribution; TauS: Tau of the stop-signal reaction time distribution; T1-T3: time points 1, 2, 3.

behavioral-only GAMMs ('nullmod'), (2) a main-effect model, ('main-slope'), in which the FD/FC regression slopes for each FBA metric were added as a fixed effect; and lastly, (3) an age-by-FD/FC interaction ('interslope'). This latter interaction model was employed to examine whether developmental improvements in response inhibition were associated with maturation of fronto-basal-ganglia white matter. SES was included as a covariate of no interest, whilst between-subject differences were entered in as random effects. We also included scanner type in these models to account for scanner upgrade.

Table 2
Summary characteristics for demographic and SST variables in the neuroimaging sample (N = 73).

	T1 (n = 38)	T2 (n = 51)	T3 (n = 27)
Demographics			
Sex, % female	32	45	33
Hand, % right	79	86	89
Age, mean (SD)	10.4 (0.5)	11.8 (0.5)	13.0 (0.5)
IQ, mean (SD)	102.1 (12.2)	100.1 (12.7)	102.8 (11.1)
SES, mean (SD)	1026 (45)	1022 (48)	1018 (42)
SST performance (ms)			
muS, mean (SD)	158.98 (72.22)	141.06 (40.51)	142.15 (34.39)
sigmaS, mean (SD)	200.02 (94.02)	144.43 (90.24)	141.63 (94.22)
tauS, mean (SD)	153.58 (62.91)	112.95 (56.95)	100.66 (50.14)
SSRT, mean (SD)	330.37 (110.93)	267.64 (73.84)	255.95 (49.13)

Note: IQ: Intelligence Quotient; SES: Socioeconomic status; SSRT: Stop-signal reaction time; MuS: Mu of the stop-signal reaction time distribution; SigmaS: Sigma of the stop-signal reaction time distribution; TauS: Tau of the stop-signal reaction time distribution; T1-T3: time points 1, 2, 3.

3. Results

3.1. Descriptive analysis

Summary statistics for the behavioral and neuroimaging samples are presented in Tables 1–3 respectively.

3.2. Primary analyses

3.2.1. Developmental trajectories of SST performance

Results of our behavioral analysis revealed a significant age-effect for SSRT (Fig. 4, panel A, $p < .001$), meaning that inhibitory control improved as children get older. However, when we explored the individual parameters to determine the drivers of this effect, we found similar age-related improvements for sigmaS (Fig. 4, panel C, $p = .004$) and tauS (Fig. 4, panel D, $p < .001$) but not for muS (Fig. 4, panel B). Overall, results indicate that reductions in the variability in stopping performance and propensity to engage in extreme responses are the primary drivers of age-related improvements in SSRT. The age models did not improve after the addition of sex or a sex-by-age interaction, suggesting that sex did not significantly contribute to individual changes in response inhibition. Parametric and smooth coefficients for all significant models are presented in Table 4. For model comparison details, refer to Tables S3-S6 in Appendix B.

3.2.2. Developmental trajectories of fronto-basal-ganglia white matter organization

GAMMs revealed that the age model was the best-fitting model for analyses involving FC (Fig. 5). In the left hemisphere, examination of the best-fitting models demonstrated significant age-related linear increases in mean logFC within the IFG-preSMA (Fig. 5, panel A, $p_{FDR} < 0.001$), and preSMA-STN (Fig. 5, panel B, $p_{FDR} < 0.001$) pathways. In the right hemisphere, we also observed significant age-related increases in logFC

Table 3
Summary characteristics for FBA measures in the neuroimaging sample (N = 73).

	T1 (n = 38)	T2 (n = 51)	T3 (n = 27)
Head Motion and Total brain volume			
FWD, mean (SD)	0.99 (0.25)	0.80 (0.12)	1.03 (0.18)
eTIV, mean (SD)	1,634,084.47 (117,478.36)	1,592,624.901 (143,446.06)	159,3501.27 (136,787.34)
Left Hemisphere			
IFG-preSMA (FD), mean (SD)	0.46 (0.03)	0.46 (0.03)	0.48 (0.03)
IFG-preSMA (logFC), mean (SD)	-0.02 (0.08)	-0.02 (0.07)	0.04 (0.10)
IFG-STN (FD), mean, (SD)	0.44 (0.03)	0.44 (0.03)	0.45 (0.03)
IFG-STN (logFC), mean, (SD)	0.07 (0.07)	0.06 (0.09)	0.08 (0.09)
preSMA-STN (FD), mean (SD)	0.61 (0.03)	0.61 (0.03)	0.62 (0.03)
preSMA-STN (logFC), mean (SD)	-0.03 (0.07)	-0.03 (0.08)	0.02 (0.09)
Right Hemisphere			
IFG-preSMA (FD), mean (SD)	0.46 (0.04)	0.46 (0.04)	0.46 (0.04)
IFG-preSMA (logFC), mean (SD)	-0.01 (0.08)	-0.02 (0.09)	0.01 (0.10)
IFG-STN (FD), mean (SD)	0.50 (0.03)	0.50 (0.03)	0.50 (0.03)
IFG-STN (logFC), mean (SD)	0.06 (0.09)	0.03 (0.09)	0.07 (0.09)
preSMA-STN (FD), mean (SD)	0.63 (0.03)	0.63 (0.03)	0.63 (0.03)
preSMA-STN (logFC), mean (SD)	-0.03 (0.06)	-0.02 (0.08)	-0.001 (0.08)

Note: FWD: Mean framewise displacement; eTIV: Estimated total intracranial volume; Left/Right IFG-preSMA (FD/logFC): Fiber density/log-transformed fiber cross-section of the left/right inferior frontal-gyrus to presupplementary motor area connection; Left/Right preSMA-STN (FD/logFC): Fiber density/log-transformed fiber cross-section of the left presupplementary motor area to subthalamic nucleus connection; Left/Right IFG-STN (FD/logFC): Fiber density/log-transformed fiber cross-section of the right inferior frontal-gyrus to presupplementary motor area connection; T1-T3: Time points 1, 2, 3.

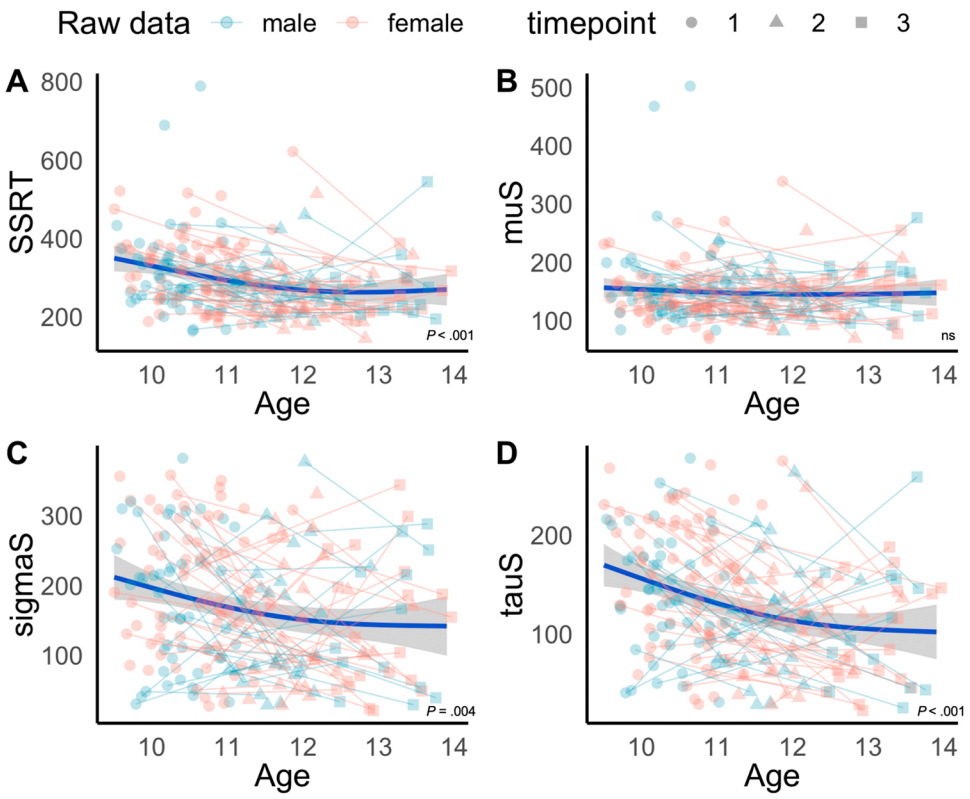

Fig. 4. Developmental trajectories of stop-signal performance across ages 9–14. Panels A-D present the best-fitting models for SSRT, muS, sigmaS and tauS respectively. Fitted lines with 95 % confidence intervals were modelled by the best fitting GAMMs for each variable of interest and overlaid on the raw data points. SSRT: Stop-signal reaction time; muS: Mu of the stop-signal reaction time distribution; sigmaS: Sigma of the stop-signal reaction time distribution; tauS: Tau of the stop-signal reaction time distribution. ns: non-significant. Age in years, SST metrics in milliseconds.

Table 4
Model coefficients for the best-fitting behavioral models.

	SSRT			SigmaS			TauS		
Parametric coefficients	*Est. (SE)*	*t*	*p*	*Est. (SE)*	*t*	*p*	*Est. (SE)*	*t*	*p*
Intercept	293.89 (7.37)	39.90	< 0.001	169.04 (6.98)	24.20	< 0.001	130.26 (4.69)	27.78	< 0.001
SES_c	-0.06 (0.17)	-0.33	0.742	0.09 (0.16)	0.55	0.584	-0.04 (0.11)	-0.36	0.719
Smooth terms	***edf (Ref.df)***	***F***	***p***	***edf (Ref.df)***	***F***	***p***	***edf (Ref.df)***	***F***	***p***
s(age_c)	2.04 (2.34)	10.09	< 0.001	1.68 (2)	5.60	0.004	1.83 (2.15)	12.03	< 0.001
s(SID)	80.04 (136)	1.44	< 0.001	41.14 (136)	0.46	0.006	58.61 (136)	0.80	< 0.001

Note: Est.: Estimated regression parameter; SE: Standard error; edf: Estimated degrees of freedom; Ref.df: Reference degrees of freedom; s(age_c): Smoothed mean-centred age; SES_c: Mean-centred SES; s (SID): Subject ID entered as a random effect. SSRT: Stop-signal reaction time; sigmaS: Sigma of the stop-signal reaction time distribution; TauS: tau of the stop-signal reaction time distribution.

of the IFG-preSMA (Fig. 5, panel D, p_{FDR} <0.001) and preSMA-STN (Fig. 5, panel E, p_{FDR} <0.001) pathways. In addition, model comparisons revealed that the age-by-sex interaction model was best-fitting for logFC in the left IFG-STN (Fig. 5, panel C), while the age-model was the best-fitting for the right IFG-STN (Fig. 5, panel F), however, these effects did not survive when correcting for multiple comparisons. Refer to Appendix B Tables S10-S12 and S16–S18 for model comparisons involving FC in the left and right hemisphere respectively. Further, we did not find any significant longitudinal associations for FD in any of the models assessed (See Appendix B Tables S7-S9 & S13–S15 for model comparisons in the left and right hemispheres respectively). Overall, results show that macrostructural properties of select tracts within the fronto-basal-ganglia circuit increases during the transition from childhood to adolescence. Parametric and smooth coefficients for all significant models are presented in Table 5 (right hemisphere) & Table 6 (left hemisphere).

3.2.3. Associations between Fronto-basal-ganglia white matter and SST performance

Extending best fitting models from 3.2.1, the addition of age-related changes in FC in the left and right IFG-preSMA and preSMA-STN pathways did not significantly improve the best-fitting models of SSRT, sigmaS and tauS (see Tables S19-S30 in Appendix B for model comparison details).

4. Discussion

The current study leverages state-of-the-art approaches in cognitive modelling and diffusion MRI to examine the development of response inhibition and fronto-basal-ganglia white matter in childhood. Building on previous cross-sectional and longitudinal work, our study used longitudinal data to demonstrate an effect of age for inhibitory performance, with faster SSRTs associated with increasing age. When using the parametric race model, these age effects on SSRT were mirrored in age effects for models of sigmaS and tauS but not muS, suggesting that SSRT development may be related to decreases in performance variability and propensity to respond very late on stop-trials. When examining the developmental progression of fronto-basal-ganglia white matter, we found significant age-related increases in fiber bundle macrostructure (indexed as FC) in the bilateral IFG-preSMA, and preSMA-STN

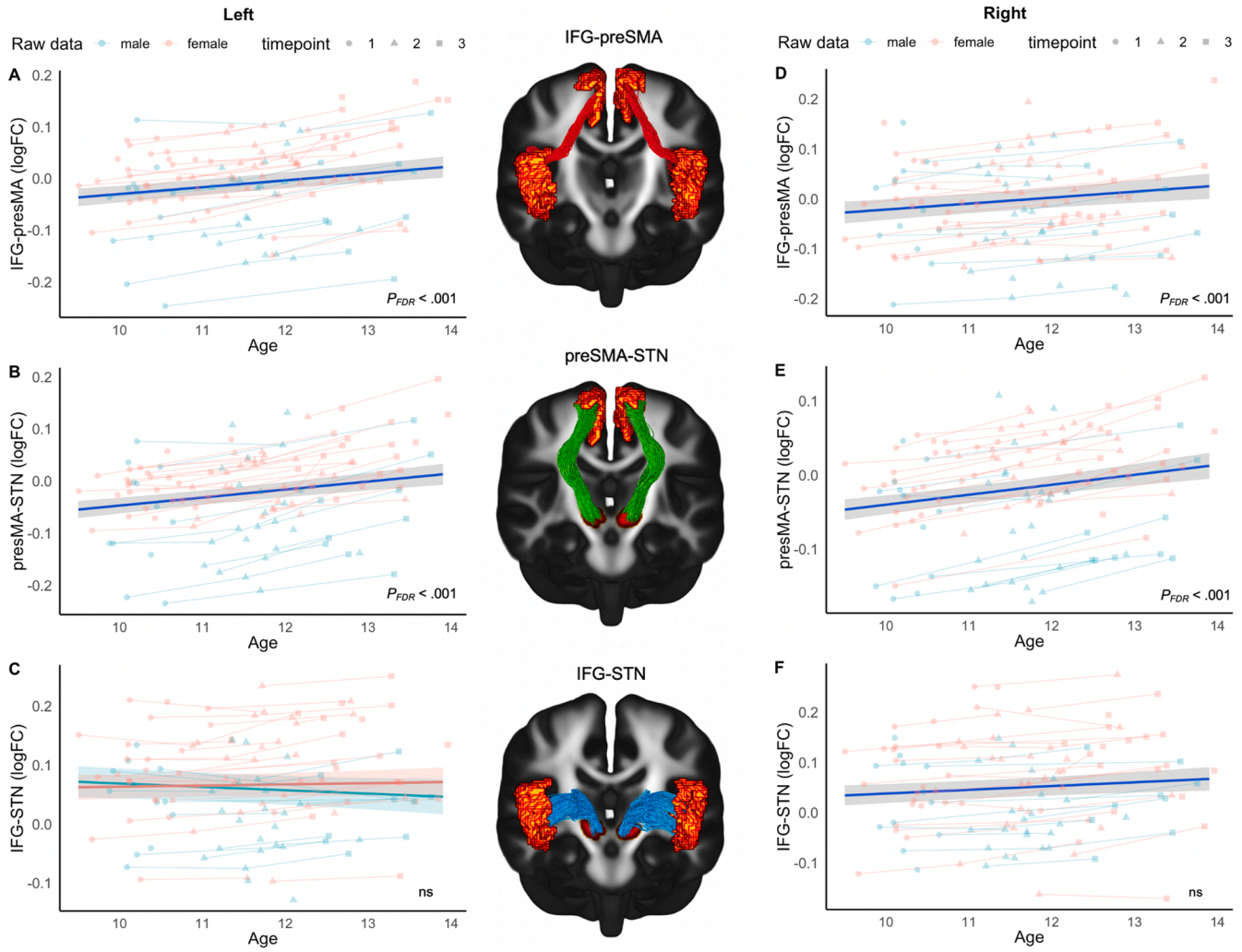

Fig. 5. Developmental trajectories of logFC underlying the fronto-basal-ganglia circuit. Panels A-C presents the best-fitting models for the left IFG-preSMA, right preSMA-STN & right IFG-STN pathways. Panels D-F presents the best-fitting models for the right IFG-preSMA, left preSMA-STN & left IFG-STN pathways. Fitted lines with 95 % confidence intervals were modelled by the best fitting GAMMs for each variable of interest and overlaid on the raw data points. Left/Right IFG-preSMA (logFC): Log-transformed fiber cross-section of the left/right inferior frontal-gyrus to presupplementary motor area connection; Left/Right preSMA-STN (logFC): Log-transformed fiber cross-section of the left/right presupplementary motor area to subthalamic nucleus connection; Left/Right IFG-STN (logFC): Log-transformed fiber cross-section of the left/right inferior frontal-gyrus to subthalamic nucleus connection. ns: non-significant.

pathways. Lastly, our combined analysis demonstrated that average change in FC did not significantly predict age-related improvements in inhibitory control. Overall, the present work improves our understanding of the underlying developmental patterns subserving childhood response inhibition. Firstly, it sheds light on the important role of performance variability and propensity to engage in very late responses towards inhibitory performance development. Second, it is the first to date that has charted the longitudinal progression of fronto-basal-ganglia white matter using a fiber-specific framework. Lastly, no significant relationship was found between changes in FC and SST metrics, suggesting that the development of white matter organization of the fronto-basal-ganglia and stopping performance follow distinct maturational trajectories.

Our longitudinal investigation of response inhibition development demonstrated significant age-related improvements in SSRT, a finding that is consistent with the existing developmental literature (Curley et al., 2018; Dupuis et al., 2019; Madsen et al., 2020; Williams et al., 1999). Like previous work, we observed a curvilinear relationship between SSRT and age, in which improvements in inhibitory control reached a plateau at around 12 years of age. Taken together, these findings support previous interpretations of inhibitory control rapidly maturing during childhood and reaching a developmental peak in the preadolescent to adolescent years (Curley et al., 2018; Dupuis et al., 2019; Madsen et al., 2020; Williams et al., 1999).

Application of the novel parametric race-model (Matzke et al., 2013) revealed complementary age-related reductions in the variability of the inhibitory response (sigmaS), and the propensity to inhibit much later during stop-trials (tauS). Several other cognitive processes (i.e. attentional orienting, stimulus detection) are also evidenced to be involved in the ability to inhibit a motor response, with successful stopping being contingent on the relative fidelity and timing of these processes (Jana et al., 2020). Considering these findings, it is possible that slower SSRTs at earlier ages may be due to a less refined executive system, leading to more inconsistent performance (i.e., higher sigma) and a greater chance of inhibiting much later than anticipated (increased skewing of the RT distribution or higher tau). Whilst this may suggest the potential role of top-down attention or stimulus detection in facilitating inhibitory control, we did not directly assess these components in the current study. As such, such inferences about the processes underlying changes in sigma and tau are speculative. Furthermore, caution is warranted when mapping cognitive mechanisms onto parameters of the ex-gaussian distribution given the lack of clear correspondence between these two

Table 5
Model coefficients for the best-fitting GAMMs of the right fronto-basal-ganglia circuit.

Right IFG-preSMA (logFC)			
Parametric coefficients	***Est. (SE)***	***t***	p_{FDR}
Intercept	0.008 (0.011)	0.710	0.618
SES_c	0.0003 (0.0002)	1.268	0.327
FWD_c	-0.002 (0.010)	-0.23	0.848
eTIV_c	0.002 (0.0005)	3.992	0.001
OFscanner	-0.010 (0.007)	-1.400	0.270
Smooth terms	***edf (Ref.df)***	***F***	p_{FDR}
s(age_c)	1.000 (1.000)	16.489	< 0.001
s(SID)	68.805 (71.000)	64.894	< 0.001
Right preSMA-STN (logFC)			
Parametric coefficients	***Est. (SE)***	***t***	p_{FDR}
Intercept	0.002 (0.008)	0.234	0.848
SES_c	0.0002 (0.0001)	1.315	0.304
FWD_c	-0.003 (0.009)	-0.376	0.779
eTIV_c	0.002 (0.0003)	8.120	< 0.001
OFscanner	-0.020 (0.006)	-3.230	0.007
Smooth terms	***edf (Ref.df)***	***F***	p_{FDR}
s(age_c)	1.000 (1.000)	26.269	< 0.001
s(SID)	67.361 (71.000)	26.981	< 0.001

Note: Right IFG-preSMA (logFC): Log-transformed fiber cross-section of the right inferior frontal-gyrus to presupplementary motor area connection; Right preSMA-STN (logFC): Log-transformed fiber cross-section of the right presupplementary motor area to subthalamic nucleus connection; Est.: Estimated regression parameter; SE: Standard error; edf: Estimated degrees of freedom; Ref.df: Reference degrees of freedom; p_{FDR}: False Discovery Rate corrected p value; s(age_c): Smoothed mean-centred age; SES_c: Mean-centred SES; s(SID): Subject ID entered as a random effect; FWD_c: Mean-centred FWD; eTIV_c: Mean-centred eTIV; OFscanner: Ordered factor of scanner type.

Table 6
Model coefficients for the best-fitting GAMMs of the left fronto-basal-ganglia circuit.

Left IFG-preSMA (logFC)			
Parametric coefficients	***Est. (SE)***	***t***	p_{FDR}
Intercept	0.023 (0.009)	2.490	0.039
SES_c	0.0002 (0.0002)	0.844	0.535
FWD_c	-0.007 (0.009)	-0.832	0.539
eTIV_c	0.002 (0.0004)	5.327	< 0.001
OFscanner	-0.031 (0.006)	-4.896	< 0.001
Smooth terms	***edf (Ref.df)***	***F***	p_{FDR}
s(age_c)	1.031 (1.061)	25.488	< 0.001
s(SID)	68.477 (71.000)	53.479	< 0.001
Left preSMA-STN (logFC)			
Parametric coefficients	***Est. (SE)***	***t***	p_{FDR}
Intercept	0.013 (0.009)	1.476	0.252
SES_c	0.0002 (0.0002)	1.056	0.424
FWD_c	0.009 (0.010)	0.952	0.474
eTIV_c	0.002 (0.0003)	6.661	< 0.001
OFscanner	-0.035 (0.007)	-5.187	< 0.001
Smooth terms	***edf (Ref.df)***	***F***	p_{FDR}
s(age_c)	1.000 (1.001)	32.095	< 0.001
s(SID)	67.932 (71.000)	37.538	< 0.001

Note: Left IFG-preSMA (logFC): Log-transformed fiber cross-section of the left inferior frontal-gyrus to presupplementary motor area connection; Left preSMA-STN (logFC): Log-transformed fiber cross-section of the left presupplementary motor area to subthalamic nucleus connection; Est.: Estimated regression parameter; SE: Standard error; edf: Estimated degrees of freedom; Ref.df: Reference degrees of freedom; p_{FDR}: False Discovery Rate corrected p value; s(age_c): Smoothed mean-centred age; SES_c: Mean-centred SES; s(SID): Subject ID entered as a random effect; FWD_c: Mean-centred FWD; eTIV_c: Mean-centred eTIV; OFscanner: Ordered factor of scanner type.

components (see Matzke and Wagenmakers, 2009; Rieger and Miller, 2020). To address this implication, future research should seek correlate these indices to performance on tasks traditionally thought to probe attention (i.e., sustained attention to response task). Nevertheless, the use of the parametric race-model constitutes a key strength of the present work as it allows us to disentangle components of the SSRT distribution that drive inter-individual performance differences in response inhibition More specifically, it calls into question the viability of single SSRT estimates as a behavioral marker of assessing developmental improvements in inhibitory control.

The neuroimaging analysis revealed significant age-related increases in FC of the bilateral IFG-preSMA and preSMA-STN pathways. In the context of the FBA framework, changes in FC is commonly thought to be associated with variability in the size, density, or thickness of the myelin sheath surrounding a fiber bundle (Dhollander et al., 2021; Raffelt et al., 2017), suggesting that axonal pathways within the fronto-basal-ganglia circuit are preferentially increasing as children get older. Larger bundle size is further thought to indirectly facilitate better transmissibility of neural information across brain regions (Raffelt et al., 2017), which may suggest a possible link between greater fiber macrostructure and improvements in inhibitory performance at older ages. In contrast to FC, no significant longitudinal trajectories were observed for FD. Previous developmental work has demonstrated localized changes in FD across a wide range of associative and commissural white matter pathways, with the time course and endpoint of maturation being regionally specific (Dimond et al., 2020; Genc et al., 2018). Considering this, it is possible that the current non-significant findings may be indicative of microstructural properties within the fronto-basal-ganglia circuit having a more protracted growth rate during the transition into adolescence. Similarly, it is also likely that developmental changes occurring at the microstructural level are more subtle in this age-range compared to macrostructure. However, this assertion is speculative, and further work to explore these trajectories across a wider age-span is warranted.

Overall, our results support the general trend of brain maturation across childhood development. White matter tracts, specifically those that support higher-order cognitive functions, demonstrate rapid maturation during childhood. These changes reflect a variety of biophysical factors including synaptogenesis, myelination or increased axonal packing (Lebel et al., 2012, 2019). Indeed, a substantial body of DTI-based imaging work has shown complementary increases in white matter FA and decreases in MD from birth to adulthood (see review by Lebel et al., 2019). Similarly, FBA studies have also revealed developmental increases in FC across several major associative and commissural tracts involved in higher-order cognitive functioning, such as the superior longitudinal fasciculus (SLF; Choy et al., 2020; Genc et al., 2018, 2020). Whilst our age-effects are relatively consistent with those obtained by Madsen et al. (2020), the use of FBA provides a more biologically specific investigation of the mechanisms that contribute to childhood brain development (Dhollander et al., 2021; Raffelt et al., 2017), suggesting that the maturation of fronto-basal-ganglia white matter over years 9–14 is largely localized to macrostructural changes rather than microstructure.

Our exploratory analyses looking at sex differences separately in the behavioral and neuroimaging samples did not reveal any significant effects, indicating that response inhibition and FC within the fronto-basal-ganglia circuit may develop at the same rate for males and females during this period. To date, evidence of sex effects in childhood inhibitory control is mixed. Some studies report no significant sex differences (Madsen, 2010; Tamnes et al., 2010), whilst others demonstrate evidence of females performing better and maturing more rapidly than males (Curley et al., 2018; Madsen et al., 2020). Likewise, evidence of sex differences in white matter development are largely mixed across the

literature. Several DTI studies report earlier development of white matter organization in females, while males show more protracted changes over time (Asato et al., 2010; Seunarine et al., 2016). Others, however, report no significant sex differences during childhood and adolescence (Brouwer et al., 2012; Genc et al., 2020; Lebel and Beaulieu, 2011). Given that we adjusted for total brain volume in our analyses, our lack of sex-effects may be considered robust since potential differences in brain size between the sexes are likely accounted for. Despite the non-significant findings in the current study, further exploration of sex effects is encouraged to see if these effects replicate in future work.

Our cross-sectional FBA study of the same cohort found that faster SSRT was associated with higher FD within subcortical projections of the bilateral IFG-STN and preSMA-STN pathways (Singh et al., 2021). This led us to investigate in this paper whether the rate of change in white matter is related to inhibition performance. Given that we found an age effect for FC in our neuroimaging analysis, we examined whether the addition of FC slope predicted changes in SST performance. Contrary to expectations, maturational changes in FC of the bilateral IFG-preSMA and preSMA-STN pathways did not predict values of sigmaS, tauS, or SSRT. That is, no significant main effects of FC slope or age-by-FC slope interactions were observed to explain SST metrics over time. The lack of significant findings regarding the relationship between changes in FC slope and SST performance may speak to the issues in attempting to model nonlinear changes in SST performance with linear changes in white matter. Further, as will be detailed in the Limitations and future recommendations (Section 4.1), our use of tract-averaged values may be insensitive at identifying the subtle associations between SST performance and white matter macrostructure. However, it is also possible that these two processes may develop distinctly during childhood. Overall, the current work suggests that the rate of change in FC of the fronto-basal-ganglia circuit over the transition to adolescence may not be indicative of an individual's overall inhibitory ability. More specifically, our results stand in contrast to those observed by Madsen et al. (2020), in which improvements in SSRT were found to be contingent on the degree of change in FA underlying the right preSMA. Nevertheless, it can be argued that the use of more specific behavioral and neuroimaging measures provides a stronger account of the nature of the relationship between brain structure and inhibitory function. Future work should seek to replicate these results to examine if these current effects hold up in other samples.

4.1. Limitations and future recommendations

Current findings should be considered in light of some limitations. Despite the advantages of using fiber-specific indices of white matter, the longitudinal FBA pipeline currently lacks the capability to conduct analyses in data acquired across more than two time points. Therefore, developmental changes in the fronto-basal-ganglia circuit were instead modelled using tract-averaged FBA values rather than at the fixel level, thus limiting the local specificity to which effects can be detected within a tract (as these were averaged across the entire tract). This lack of specificity may be a reason for why we did not observe significant age-effects for FD in our sample. Similarly, our study was impacted by attrition, resulting in an unbalanced dataset across the three time points. However, a key strength of our study was the use of GAMMs which is robust to the presence of missing data, therefore allowing us to utilize our full longitudinal dataset in our analyses (Hastie and Tibshirani, 1990).

Looking to future work, although white matter properties of the fronto-basal-ganglia circuit have been associated with inhibitory control across much of the stop-signal literature (Aron et al., 2016, 2007; Chen, 2020; Coxon et al., 2012; Madsen, 2010; Madsen et al., 2020; Rae et al., 2015; Singh et al., 2021), the specific role of each region within the fronto-basal-ganglia circuit remains a point of contention (e.g., see Aron et al., 2014; Hampshire, 2015; Hampshire et al., 2010). Indeed, the frontoparietal regions subserve several goal-directed cognitive and affective functions beyond inhibition (Friedman and Robbins, 2021). Furthermore, there is substantial overlap between axonal fibers of the fronto-basal-ganglia circuit with those of other frontostriatal tracts that have been implicated in higher-order executive functioning, such as the SLF (Chiang et al., 2015). Given that we found evidence to suggest that other non-inhibitory processes may indeed subserve response inhibition development (cf. sigma and tau), this could imply that the performance variability and long infrequent responses (contributing to longer SSRTs) may be better captured by these other higher-order white matter tracts proximal to the fronto-basal-ganglia circuit. To understand the specificity of our findings, it is recommended for future work to explore whether variability in sigma or tau would be significantly associated with the developmental trajectories of tracts traditionally identified as subserving other executive functions.

4.2. Conclusions

In this study, we examined the developmental trajectories of response inhibition, fronto-basal-ganglia white matter, and the associations between both measures in a cohort of typically developing children aged 9–14 years. We observed a significant improvement in inhibitory control as children got older, an effect which was explained by a reduction in variability and skewness of the SSRT distribution. By applying fiber-specific indices of white matter organization, we revealed that the development of the fronto-basal-ganglia circuit in children is largely confined to changes in fiber macrostructure rather than microstructure of the bilateral IFG-preSMA and preSMA-STN pathways. Inconsistent with our hypothesis, we did not find any meaningful associations between response inhibition and age-related improvements in FC of the bilateral IFG-preSMA and preSMA-STN pathways. Taken together, the present study sheds light on the likely cognitive mechanisms subserving inhibitory control development in children, and the maturational trajectories of fronto-basal-ganglia macrostructure.

CRediT authorship contribution statement

Mervyn Singh: Conceptualization; Methodology; Formal Analysis; Writing – original draft; Writing – review & editing. **Patrick Skippen:** Methodology; Formal analysis; Writing – review & editing. **Jason He:** Methodology; Writing – review & editing. **Phoebe Thomson:** Methodology; Formal analysis; Writing – review & editing. **Ian Fuelscher:** Supervision; Conceptualization; Methodology; Writing – original draft; Writing – review & editing. **Karen Caeyenberghs:** Methodology; Writing – review & editing. **Vicki Anderson:** Writing – review & editing. **Jan M. Nicholson:** Writing – review & editing. **Christian Hyde:** Supervision; Conceptualization; Methodology; Writing – original draft; Writing – review & editing. **Timothy J. Silk:** Supervision; Conceptualization; Project Administration; Funding acquisition; Methodology; Writing – original draft; Writing – review & editing.

Declaration of Competing Interest

The authors declare that they have no known competing financial interests or personal relationships that could have appeared to influence the work reported in this paper.

Data Availability

Data from the Children's Attention Project cohort are available via Lifecourse: https://lifecourse.melbournechildrens.com/cohorts/capnicap/. All code used for statistical analysis, as well as group-averaged tracts, are publicly available on GitHub: https://github.com/MervSingh/Longitudinal_FBA_SST.git.

Acknowledgements

The study was conducted in accordance with the guidelines for human research set out in the Declaration of Helsinki. This study was funded by the Australian National Medical Health and Research Council (NHMRC; project grant #1065895). Ethics approval was granted by the Royal Children's Hospital Human Research Ethics Committee, Melbourne (#34071). MS is supported by a Postgraduate Research Scholarship from Deakin University, Melbourne. This work was also supported by computational resources provided by the Australian Government through MASSIVE under the National Computational Merit Allocation Scheme. We would like to extend our gratitude to the Royal Children's Hospital medical staff for their expertise in the collection of neuroimaging data, and the researchers involved in the collection of behavioral measures used in the present study. Lastly, we would like to thank all parents, guardians, and their children for their participation in this study.

Appendix A and B. Supporting information

Supplementary data associated with this article can be found in the online version at doi:10.1016/j.dcn.2022.101171.

References

Anzman-Frasca, S., Francis, L.A., Birch, L.L., 2015. Inhibitory control is associated with psychosocial, cognitive, and weight outcomes in a longitudinal sample of girls. Transl. Issues Psychol. Sci., Psychol. Adv. Obes. 1, 203–216. https://doi.org/10.1037/tps0000028.

Aron, A.R., Behrens, T.E., Smith, S., Frank, M.J., Poldrack, R.A., 2007. Triangulating a cognitive control network using diffusion-weighted magnetic resonance imaging (MRI) and functional MRI. J. Neurosci. 27, 3743–3752. https://doi.org/10.1523/JNEUROSCI.0519-07.2007.

Aron, A.R., Robbins, T.W., Poldrack, R.A., 2014. Right inferior frontal cortex: addressing the rebuttals. Front Hum. Neurosci. 8. https://doi.org/10.3389/fnhum.2014.00905.

Aron, A.R., Herz, D.M., Brown, P., Forstmann, B.U., Zaghloul, K., 2016. Frontosubthalamic circuits for control of action and cognition. J. Neurosci. 36. https://doi.org/10.1523/JNEUROSCI.2348-16.2016.

Asato, M.R., Terwilliger, R., Woo, J., Luna, B., 2010. White matter development in adolescence: a DTI study. Cereb. Cortex 20, 2122–2131. https://doi.org/10.1093/cercor/bhp282.

Australian Bureau of Statistics, 2013. Census of population and housing: socio-economic indexes for areas (SEIFA), Australia, 2011. cat. no. 2033.0. 55.001 https://www.abs.gov.au/ausstats/abs@.nsf/DetailsPage/2033.0.55.0012011. ABS, Canberra.

Bari, A., Robbins, T.W., 2013. Inhibition and impulsivity: behavioral and neural basis of response control. Prog. Neurobiol. 108. https://doi.org/10.1016/j.pneurobio.2013.06.005.

Bedard, A.-C., Nichols, S., Barbosa, J.A., Schachar, R., Logan, G.D., Tannock, R., 2002. The development of selective inhibitory control across the life span. Dev. Neuropsychol. 21, 93–111. https://doi.org/10.1207/S15326942DN2101_5.

Benjamini, Y., Hochberg, Y., 1995. Controlling the false discovery rate: a practical and powerful approach to multiple testing. J. R. Stat. Soc. Ser. B Methodol. 57, 289–300. https://doi.org/10.1111/j.2517-6161.1995.tb02031.x.

Brouwer, R.M., Mandl, R.C.W., Schnack, H.G., Soelen, I.L.C., van, Baal, G.C., van, Peper, J.S., Kahn, R.S., Boomsma, D.I., Pol, H.E.H., 2012. White matter development in early puberty: a longitudinal volumetric and diffusion tensor imaging twin study. PLOS ONE 7, e32316. https://doi.org/10.1371/journal.pone.0032316.

Chen, W., 2020. Prefrontal-subthalamic hyperdirect pathway modulates movement inhibition in humans. Neuron 106. https://doi.org/10.1016/j.neuron.2020.02.012.

Chiang, H.-L., Chen, Y.-J., Lo, Y.-C., Tseng, W.-Y.I., Gau, S.S.-F., 2015. Altered white matter tract property related to impaired focused attention, sustained attention, cognitive impulsivity and vigilance in attention-deficit/hyperactivity disorder. J. Psychiatry Neurosci. JPN 40, 325–335. https://doi.org/10.1503/jpn.140106.

Choy, S.W., Bagarinao, E., Watanabe, H., Ho, E.T.W., Maesawa, S., Mori, D., Hara, K., Kawabata, K., Yoneyama, N., Ohdake, R., Imai, K., Masuda, M., Yokoi, T., Ogura, A., Taoka, T., Koyama, S., Tanabe, H.C., Katsuno, M., Wakabayashi, T., Kuzuya, M., Hoshiyama, M., Isoda, H., Naganawa, S., Ozaki, N., Sobue, G., 2020. Changes in white matter fiber density and morphology across the adult lifespan: a cross-sectional fixel-based analysis. Hum. Brain Mapp. 41, 3198–3211. https://doi.org/10.1002/hbm.25008.

Coxon, J.P., Van Impe, A., Wenderoth, N., Swinnen, S.P., 2012. Aging and inhibitory control of action: cortico-subthalamic connection strength predicts stopping performance. J. Neurosci. 32, 8401–8412. https://doi.org/10.1523/JNEUROSCI.6360-11.2012.

Curley, L.B., Newman, E., Thompson, W.K., Brown, T.T., Hagler Jr., D.J., Akshoomoff, N., Reuter, C., Dale, A.M., Jernigan, T.L., 2018. Cortical morphology of the pars opercularis and its relationship to motor-inhibitory performance in a longitudinal, developing cohort. Brain Struct. Funct. 223, 211–220. https://doi.org/10.1007/s00429-017-1480-5.

Dawson, M.R.W., 1988. Fitting the ex-Gaussian equation to reaction time distributions. Behav. Res. Methods Instrum. Comput. 20, 54–57. https://doi.org/10.3758/BF03202603.

Dell'Acqua, F., Tournier, J.D., 2019. Modelling white matter with spherical deconvolution: How and why? NMR Biomed. 32, e3945 https://doi.org/10.1002/nbm.3945.

Dhollander, T., Connelly, A., 2016. A novel iterative approach to reap the benefits of multi-tissue CSD from just single-shell (+ b= 0) diffusion MRI data. Presented at the Proc ISMRM, p. 3010.

Dhollander, T., Clemente, A., Singh, M., Boonstra, F., Civier, O., Duque, J.D., Egorova, N., Enticott, P., Fuelscher, I., Gajamange, S., Genc, S., Gottlieb, E., Hyde, C., Imms, P., Kelly, C., Kirkovski, M., Kolbe, S., Liang, X., Malhotra, A., Mito, R., Poudel, G., Silk, T.J., Vaughan, D.N., Zanin, J., Raffelt, D., Caeyenberghs, K., 2021. Fixel-based Analysis of diffusion MRI: methods, applications, challenges and opportunities. NeuroImage 241, 118417. https://doi.org/10.1016/j.neuroimage.2021.118417.

Diesburg, D.A., Wessel, J.R., 2021. The Pause-then-Cancel model of human action-stopping: theoretical considerations and empirical evidence. S0149763421003183 Neurosci. Biobehav. Rev.. https://doi.org/10.1016/j.neubiorev.2021.07.019.

Dimond, D., Rohr, C.S., Smith, R.E., Dhollander, T., Cho, I., Lebel, C., Dewey, D., Connelly, A., Bray, S., 2020. Early childhood development of white matter fiber density and morphology. NeuroImage 210, 116552. https://doi.org/10.1016/j.neuroimage.2020.116552.

Dupuis, A., Indralingam, M., Chevrier, A., Crosbie, J., Arnold, P., Burton, C.L., Schachar, R., 2019. Response time adjustment in the stop signal task: development in children and adolescents. Child Dev. 90, e263–e272. https://doi.org/10.1111/cdev.13062.

Farquharson, S., Tournier, J.D., Calamante, F., Fabinyi, G., Schneider-Kolsky, M., Jackson, G.D., Connelly, A., 2013. White matter fiber tractography: why we need to move beyond DTI. J. Neurosurg. 118, 1367–1377. https://doi.org/10.3171/2013.2.JNS121294.

Friedman, N.P., Robbins, T.W., 2021. The role of prefrontal cortex in cognitive control and executive function. Neuropsychopharmacology 1–18. https://doi.org/10.1038/s41386-021-01132-0.

Genc, S., Smith, R.E., Malpas, C.B., Anderson, V., Nicholson, J.M., Efron, D., Sciberras, E., Seal, M.L., Silk, T.J., 2018. Development of white matter fibre density and morphology over childhood: A longitudinal fixel-based analysis. NeuroImage 183, 666–676. https://doi.org/10.1016/j.neuroimage.2018.08.043.

Genc, S., Malpas, C.B., Gulenc, A., Sciberras, E., Efron, D., Silk, T.J., Seal, M.L., 2020. Longitudinal patterns of white matter fibre density and morphology in children are associated with age and pubertal stage. Dev. Cogn. Neurosci. 45, 100853 https://doi.org/10.1016/j.dcn.2020.100853.

Gibbons, R.D., Hedeker, D., DuToit, S., 2010. Advances in analysis of longitudinal data. Annu. Rev. Clin. Psychol. 6, 79–107. https://doi.org/10.1146/annurev.clinpsy.032408.153550.

Goscinski, W.J., McIntosh, P., Felzmann, U., Maksimenko, A., Hall, C.J., Gureyev, T., Thompson, D., Janke, A., Galloway, G., Killeen, N.E.B., Raniga, P., Kaluza, O., Ng, A., Poudel, G., Barnes, D.G., Nguyen, T., Bonnington, P., Egan, G.F., 2014. The multi-modal Australian sciences imaging and visualization Environment (MASSIVE) high performance computing infrastructure: applications in neuroscience and neuroinformatics research. Front. Neuroinformatics 8, 30. https://doi.org/10.3389/fninf.2014.00030.

Hampshire, A., 2015. Putting the brakes on inhibitory models of frontal lobe function. NeuroImage 113, 340–355. https://doi.org/10.1016/j.neuroimage.2015.03.053.

Hampshire, A., Chamberlain, S.R., Monti, M.M., Duncan, J., Owen, A.M., 2010. The role of the right inferior frontal gyrus: Inhibition and attentional control. NeuroImage 50, 1313–1319. https://doi.org/10.1016/j.neuroimage.2009.12.109.

Hannah, R., Aron, A.R., 2021. Towards real-world generalizability of a circuit for action-stopping. Nat. Rev. Neurosci. 1–15. https://doi.org/10.1038/s41583-021-00485-1.

Hastie, T.J., Tibshirani, R.J., 1990. Generalized Additive Models. CRC press.

Jana, S., Hannah, R., Muralidharan, V., Aron, A.R., 2020. Temporal cascade of frontal, motor and muscle processes underlying human action-stopping. eLife 9. https://doi.org/10.7554/eLife.50371.

Jeurissen, B., Leemans, A., Tournier, J.-D., Jones, D.K., Sijbers, J., 2013. Investigating the prevalence of complex fiber configurations in white matter tissue with diffusion magnetic resonance imaging. Hum. Brain Mapp. 34, 2747–2766. https://doi.org/10.1002/hbm.22099.

Last, B.S., Lawson, G.M., Breiner, K., Steinberg, L., Farah, M.J., 2018. Childhood socioeconomic status and executive function in childhood and beyond. PLOS ONE 13, e0202964. https://doi.org/10.1371/journal.pone.0202964.

Lawson, G.M., Hook, C.J., Farah, M.J., 2018. A meta-analysis of the relationship between socioeconomic status and executive function performance among children. Dev. Sci. 21, e12529 https://doi.org/10.1111/desc.12529.

Lebel, C., Beaulieu, C., 2011. Longitudinal development of human brain wiring continues from childhood into adulthood. J. Neurosci. 31, 10937–10947. https://doi.org/10.1523/JNEUROSCI.5302-10.2011.

Lebel, C., Gee, M., Camicioli, R., Wieler, M., Martin, W., Beaulieu, C., 2012. Diffusion tensor imaging of white matter tract evolution over the lifespan. NeuroImage 60, 340–352. https://doi.org/10.1016/j.neuroimage.2011.11.094.

Lebel, C., Treit, S., Beaulieu, C., 2019. A review of diffusion MRI of typical white matter development from early childhood to young adulthood. NMR Biomed. 32, e3778 https://doi.org/10.1002/nbm.3778.

Lewis, F., Butler, A., Gilbert, L., 2011. A unified approach to model selection using the likelihood ratio test. Methods Ecol. Evol. 2, 155–162. https://doi.org/10.1111/j.2041-210X.2010.00063.x.

Lipszyc, J., Schachar, R., 2010. Inhibitory control and psychopathology: a meta-analysis of studies using the stop signal task. J. Int. Neuropsychol. Soc. 16, 1064–1076. https://doi.org/10.1017/S1355617710000895.

Logan, G.D., Cowan, W.B., 1984. On the ability to inhibit thought and action: a theory of an act of control. Psychol. Rev. 91, 295–327. https://doi.org/10.1037/0033-295X.91.3.295.

Madsen, K.S., 2010. Response inhibition is associated with white matter microstructure in children. Neuropsychologia 48. https://doi.org/10.1016/j.neuropsychologia.2009.11.001.

Madsen, K.S., Johansen, L.B., Thompson, W.K., Siebner, H.R., Jernigan, T.L., Baaré, W.F. C., 2020. Maturational trajectories of white matter microstructure underlying the right presupplementary motor area reflect individual improvements in motor response cancellation in children and adolescents. NeuroImage 220. https://doi.org/10.1016/j.neuroimage.2020.117105.

Matzke, D., Wagenmakers, E.-J., 2009. Psychological interpretation of the ex-Gaussian and shifted Wald parameters: a diffusion model analysis. Psychon. Bull. Rev. 16, 798–817. https://doi.org/10.3758/PBR.16.5.798.

Matzke, D., Dolan, C.V., Logan, G.D., Brown, S.D., Wagenmakers, E.-J., 2013. Bayesian parametric estimation of stop-signal reaction time distributions. J. Exp. Psychol. Gen. 142, 1047–1073. https://doi.org/10.1037/a0030543.

Matzke, D., Verbruggen, F., Logan, G.D., 2018. The stop-signal paradigm, in: stevens' handbook of experimental psychology and cognitive Neuroscience. Am. Cancer Soc. 1–45. https://doi.org/10.1002/9781119170174.epcn510.

Matzke, D., Curley, S., Gong, C.Q., Heathcote, A., 2019. Inhibiting responses to difficult choices. J. Exp. Psychol. Gen. 148, 124–142. https://doi.org/10.1037/xge0000525.

O'Donnell, L.J., Westin, C.F., 2011. An introduction to diffusion tensor image analysis. Neurosurg. Clin. N. Am. 22, 185–196. https://doi.org/10.1016/j.nec.2010.12.004.

Portet, S., 2020. A primer on model selection using the Akaike Information criterion. Infect. Dis. Model. 5, 111–128. https://doi.org/10.1016/j.idm.2019.12.010.

Power, J.D., Barnes, K.A., Snyder, A.Z., Schlaggar, B.L., Petersen, S.E., 2012. Spurious but systematic correlations in functional connectivity MRI networks arise from subject motion. NeuroImage 59, 2142–2154. https://doi.org/10.1016/j.neuroimage.2011.10.018.

Rae, C.L., Hughes, L.E., Anderson, M.C., Rowe, J.B., 2015. The prefrontal cortex achieves inhibitory control by facilitating subcortical motor pathway connectivity. J. Neurosci. 35. https://doi.org/10.1523/JNEUROSCI.3093-13.2015.

Raffelt, D., Tournier, J.D., Rose, S., Ridgway, G.R., Henderson, R., Crozier, S., Salvado, O., Connelly, A., 2012. Apparent Fibre Density: A novel measure for the analysis of diffusion-weighted magnetic resonance images. NeuroImage 59, 3976–3994. https://doi.org/10.1016/j.neuroimage.2011.10.045.

Raffelt, D.A., Tournier, J.D., Smith, R.E., Vaughan, D.N., Jackson, G., Ridgway, G.R., Connelly, A., 2017. Investigating white matter fibre density and morphology using fixel-based analysis. NeuroImage 144, 58–73. https://doi.org/10.1016/j.neuroimage.2016.09.029.

Ribeiro, F., Cavaglia, R., Rato, J.R., 2021. Sex differences in response inhibition in young children. Cogn. Dev. 58, 101047 https://doi.org/10.1016/j.cogdev.2021.101047.

Rieger, T., Miller, J., 2020. Are model parameters linked to processing stages? an empirical investigation for the ex-Gaussian, ex-Wald, and EZ diffusion models. Psychol. Res. 84, 1683–1699. https://doi.org/10.1007/s00426-019-01176-4.

Rubia, K., Lim, L., Ecker, C., Halari, R., Giampietro, V., Simmons, A., Brammer, M., Smith, A., 2013. Effects of age and gender on neural networks of motor response inhibition: From adolescence to mid-adulthood. NeuroImage 83, 690–703. https://doi.org/10.1016/j.neuroimage.2013.06.078.

Schachar, R., Logan, G.D., Robaey, P., Chen, S., Ickowicz, A., Barr, C., 2007. Restraint and cancellation: multiple inhibition deficits in attention deficit hyperactivity disorder. J. Abnorm Child Psychol. 35, 229–238.

Seunarine, K.K., Clayden, J.D., Jentschke, S., Muñoz, M., Cooper, J.M., Chadwick, M.J., Banks, T., Vargha-Khadem, F., Clark, C.A., 2016. Sexual dimorphism in white matter developmental trajectories using tract-based spatial statistics. Brain Connect 6, 37–47. https://doi.org/10.1089/brain.2015.0340.

Silk, T.J., Genc, S., Anderson, V., Efron, D., Hazell, P., Nicholson, J.M., Kean, M., Malpas, C.B., Sciberras, E., 2016. Developmental brain trajectories in children with ADHD and controls: a longitudinal neuroimaging study. BMC Psychiatry 16, 1–9. https://doi.org/10.1186/s12888-016-0770-4.

Singh, M., Fuelscher, I., He, J., Anderson, V., Silk, T.J., Hyde, C., 2021. Inter-individual performance differences in the stop-signal task are associated with fibre-specific microstructure of the fronto-basal-ganglia circuit in healthy children. Cortex.

Skippen, P., 2019. Reliability of triggering inhibitory process is a better predictor of impulsivity than SSRT. Acta Psychol. 192. https://doi.org/10.1016/j.actpsy.2018.10.016.

Smith, R.E., Dhollander, T., Connelly, A., 2019. On the regression of intracranial volume in fixel-based. Analysis 3.

Tamnes, C.K., Østby, Y., Walhovd, K.B., Westlye, L.T., Due-Tønnessen, P., Fjell, A.M., 2010. Neuroanatomical correlates of executive functions in children and adolescents: a magnetic resonance imaging (MRI) study of cortical thickness. Neuropsychologia 48, 2496–2508. https://doi.org/10.1016/j.neuropsychologia.2010.04.024.

Tournier, J.D., Calamante, F., Connelly, A., 2007. Robust determination of the fibre orientation distribution in diffusion MRI: non-negativity constrained super-resolved spherical deconvolution. NeuroImage 35, 1459–1472. https://doi.org/10.1016/j.neuroimage.2007.02.016.

Tournier, J.D., Smith, R., Raffelt, D., Tabbara, R., Dhollander, T., Pietsch, M., Christiaens, D., Jeurissen, B., Yeh, C.-H., Connelly, A., 2019. MRtrix3: A fast, flexible and open software framework for medical image processing and visualisation. NeuroImage 202.

Van Rij, J., Wieling, M., Baayen, R.H., van Rijn, D., 2015. itsadug: Interpreting time series and autocorrelated data using GAMMs.

Verbruggen, F., Logan, G.D., 2008. Response inhibition in the stop-signal paradigm. Trends Cogn. Sci. 12, 418–424. https://doi.org/10.1016/j.tics.2008.07.005.

Verbruggen, F., Logan, G.D., 2009. Models of response inhibition in the stop-signal and stop-change paradigms. Neurosci. Biobehav. Rev., Stopping Action Cogn. 33, 647–661. https://doi.org/10.1016/j.neubiorev.2008.08.014.

Verbruggen, F., Logan, G.D., Stevens, M.A., 2008. STOP-IT: windows executable software for the stop-signal paradigm. Behav. Res. Methods 40, 479–483. https://doi.org/10.3758/BRM.40.2.479.

Verbruggen, F., Chambers, C.D., Logan, G.D., 2013. Fictitious inhibitory differences: how skewness and slowing distort the estimation of stopping latencies. Psychol. Sci. 24, 352–362. https://doi.org/10.1177/0956797612457390.

Williams, B.R., Ponesse, J.S., Schachar, R.J., Logan, G.D., Tannock, R., 1999. Development of inhibitory control across the life span. Dev. Psychol. 35, 205–213. https://doi.org/10.1037/0012-1649.35.1.205.

Wechsler, 1999. Manual for the Wechsler abbreviated intelligence scale (WASI). The Psychological Corporation, San Antonio, TX, p. 10.

Williams, B.R., Hultsch, D.F., Strauss, E.H., Hunter, M.A., Tannock, R., 2005. Inconsistency in reaction time across the life span. Neuropsychology 19, 88–96. https://doi.org/10.1037/0894-4105.19.1.88.

Wood, S.N., 2011. Fast stable restricted maximum likelihood and marginal likelihood estimation of semiparametric generalized linear models. J. R. Stat. Soc. Ser. B Stat. Method. 73, 3–36. https://doi.org/10.1111/j.1467-9868.2010.00749.x.

Wood, S.N., 2017. Generalized Additive Models: An Introduction With R. CRC press.